An innovative design for left turn bicycles at continuous flow intersections

Zhao, Jing; Gao, Xing; Knoop, Victor

DOI
10.1080/21680566.2019.1614496

Publication date
2019

Document Version
Accepted author manuscript

Published in
Transportmetrica B: Transport Dynamics

Citation (APA)
Zhao, J., Gao, X., & Knoop, V. (2019). An innovative design for left turn bicycles at continuous flow intersections. *Transportmetrica B: Transport Dynamics*, *7*(1), 1305–1322. https://doi.org/10.1080/21680566.2019.1614496

Important note
To cite this publication, please use the final published version (if applicable).
Please check the document version above.

An innovative design for left turn bicycles at continuous flow intersections

Zhao, Jing; Gao, Xing; Knoop, Victor

DOI
10.1080/21680566.2019.1614496

Publication date
2019

Document Version
Accepted author manuscript

Published in
Transportmetrica B: Transport Dynamics

Citation (APA)
Zhao, J., Gao, X., & Knoop, V. (2019). An innovative design for left turn bicycles at continuous flow intersections. *Transportmetrica B: Transport Dynamics*, *7*(1), 1305–1322. https://doi.org/10.1080/21680566.2019.1614496

Important note
To cite this publication, please use the final published version (if applicable).
Please check the document version above.

An innovative design for left turn bicycles at continuous flow intersections

Jing Zhao[a]*, Xing Gao[a] and Victor L. Knoop[b]

[a]*Department of Traffic Engineering, University of Shanghai for Science and Technology, Shanghai, China;* [b]*Transport & Planning, Delft University of Technology, Delft, Netherlands*

* Email: jing_zhao_traffic@163.com; Tel.: (8621) 6571-0430; Fax: (8621) 6571-0430

An innovative design for left turn bicycles at continuous flow intersections

To improve the practical capacity of the continuous flow intersections (CFI) and eliminate the conflict between left-turn bicycles and through vehicles at the main-signal, an optimization design method for left-turn bicycles was proposed. From the perspective of the geometric design, the pre-stop line for through vehicles and the crossing passage for left-turn bicycles were set at the pre-signal points of the CFI. From the perspective of signal control, the control of the through vehicles at pre-signal was added in the proposed method. A linear programming model was established to achieve the maximum vehicular practical capacity. The optimization effectiveness and applicability for this design were validated by a case study and sensitivity analyses. The results show that this method can effectively avoid the conflict between left-turn bicycles and through vehicles at main-signal and enhance the practical capacity at continuous flow intersections. As for vehicles, the improvements in practical capacity obtained by the proposed method increase with the increase of the left-turn bicycles volume and through vehicle percentage, while decrease with longer cycle length. On average, a 5% increase and 3.5% increase in the improvement of practical capacity can be obtained for every 100 left-turn bicycles per hour increase and for every 10% through vehicle percentage increase, respectively. As for bicycles, the proposed method can reduce the delay in the case of high traffic demand.

Keywords: continuous flow intersections; left-turn bicycles; unconventional design, practical capacity; linear programming

1. Introduction

The intersection is the bottleneck node of the urban road network. The conflict between left-turn and through vehicles is the key factor that causes the increase of vehicle delay, and the decrease of the road capacity and traffic safety (Mirheli, Hajibabai, and Hajbabaie 2018; Bagloee and Asadi 2016; Tong et al. 2015). Methods to deal with these problems have been a concern of traffic engineers for a long time, including providing exclusive left-turn lanes and left-turn waiting areas (Ma et al. 2017; Yang et al. 2013;

Zhou and Zhuang 2012; Dong et al. 2016; Yang et al. 2012) in the aspect of road layout, adding left-turn phases in the aspect of signal control (Al-Kaisy and Stewart 2001; Allsop 1971; Webster 1958; Heydecker and Dudgeon 1987; Improta and Cantarella 1984; Silcock 1997)., and prohibiting conflicting left-turns and setting detour routes in the aspect of road network organization (DePrator, Hitchcock, and Gayah 2017; Zhao, Liu, and Li 2016; Yu and Prevedouros 2013). With the increase of traffic demand, median U-turn intersections (Liu et al. 2007; El Esawey and Sayed 2011; Mohapatra and Dey 2018; Zhao et al. 2018), continuous flow intersections (Goldblatt, Mier, and Friedman 1994; Yang and Cheng 2017), exit lanes for left-turn intersections (Zhao et al. 2013; Wu et al. 2016), tandem intersections (Xuan, Daganzo, and Cassidy 2011; Ma et al. 2013; Yan, Jiang, and Xie 2014), uninterrupted flow intersections (Liu and Luo 2012; Xie and Turnquist 2011), special width approach lanes intersections (Zhao, Liu, and Wang 2016) and other series of unconventional intersection design methods have been proposed and applied in many cities all over the world, to further improve the capacity of intersections.

Among these unconventional intersection designs, the continuous flow intersection (CFI) is rapidly becoming prevalent worldwide (Jagannathan and Bared 2005). At CFI, the pre-signals are set at the upstream of the main-signals and left-turn lanes are moved to the left of the exit lanes. Thus, the conflict between the left-turn vehicles and opposite through vehicles at main-signals is transferred to the upstream pre-signals. In addition, the main-signals can run in two phases at CFI. In the development of the CFI, studies mainly contain three aspects: geometric design, signal control, and operational safety.

From the perspective of the geometric design, Jagannathan (Jagannathan and Bared 2004; Jagannathan and Bared 2005) successively analyzed left-turn traffic and

pedestrian at CFI, and then recommended the width of the displaced left-turn lanes and the design of pedestrian crossing based on the characteristics of turning radius of left-turn vehicles at the crossover and main intersection. Hildebrand (2007) recommended the angle between the left-turn lanes and the main through lanes at the crossover, and compared the performances between CFI and conventional design based on service level, area required, traffic simulation, and estimated construction cost. Hughes et al. (2010) gave a series of detailed suggestions on left-turn lane length, sub-intersection width, turning radius and other minor dimensions at continuous flow intersections. Tanwanichkul, Pitaksringkarn, and Boonchawee (2011) recommended distances between main intersection and sub-intersection for different traffic conditions based on Vissim simulation.

From the perspective of signal control, considering the complex operational process of the CFI, several special methods were proposed to optimize the signal timing and improve the efficiency of the CFI. Jagannathan and Bared (2004) broke the CFI into a group of hypothetical intersections and used the WINQSB operational research solver to solve an optimization model for the signal timing and offsets. El Esawey and Sayed (2007) divided the phase sequence of the continuous flow intersection into six parts according to its unique queuing and running characteristics. Then, commercial signal timing packages can be used to develop signal timings. Chang, Lu, and Yang (2011) built an estimation model of queuing and delay by simulating a large number of statistical data. With the objective of cycle length minimization, You, Li, and Ma (2013) proposed a model for a full continuous flow intersection (CFI) based on the analysis of the evolution process of vehicle queuing. Suh and Hunter (2014) proposed two optimization approaches for the CFI: a Monte Carlo simulation method to minimize intersection delay and a bandwidth maximization method. Results showed that the delay

and the bandwidth approaches have similar performance characteristics. Sun et al. (2015) proposed a simplified continuous flow intersection (called CFI-Lite) design. Instead of newly constructing a sub-intersection, this design used the existing upstream intersection, to allocate left-turn traffic to the left-most lane. Left-turn traffic turns to the DLT lane in advance at the upstream intersection. It can be used at arterials with closely spaced intersections. Zhao et al. (2015) established an integrated optimization model for the geometric layout and signal timing in which many key parameters, such as intersection form, lane function, left-turn lane length and signal timing, were optimized in a unified framework.

From the perspective of traffic safety, it was found that drivers had no confusion when passing the continuous flow intersections at the first time according to the driving simulator experiment conducted by Inman (2009), which proved that the design of the continuous flow intersection was also helpful to improve the intersection safety. Except for the analysis of motor vehicles, Coates et al. (2014) further proposed a crosswalk geometry and signal timing method to improve pedestrian safety at continuous flow intersections. By considering pedestrian waiting time, existing queue length and selecting green time dynamically, the pedestrian delay was minimized.

After more than 30 years of development, the CFI has been taken into application in 17 American cities since it could enhance the traffic efficiency dramatically. Recently, with the help of local government, the CFI was applicated an intersection in Shenzhen, China. However, the existing research is mainly focused on motor vehicles and the practice is also mainly applied in areas dominated by motor vehicles. In many developing countries, such as China, bicycle is also an important traffic mode. However, the conflict between left-turn bicycles and through vehicles at CFI is neglected. Therefore, under the condition of two-phase control, the operational

efficiency of vehicles will be significantly reduced and there are serious safety risks for left-turn bicycles.

Although there are abundant research achievements on geometric design (Tengattini and Bigazzi 2017; Jia, O'Mara, and Guan 2007; Providelo and Sanches 2011; Raihan and Alluri 2017; Goodno et al. 2013), signal control (Kothuri et al. 2017; Portilla et al. 2016; Thompson et al. 2013) and level of service evaluation (Majumdar and Mitra 2018; Foster et al. 2015; Bai et al. 2017) of bicycles at conventional intersections, lacking improvement measures to eliminate the conflicts between left-turn bicycles and through vehicles for CFI limits its applicability, especially in developing countries.

In this paper, an optimization design method for left-turn bicycles at CFI was proposed to eliminate the conflict between left-turn bicycles and through vehicles at the main-signals, including the aspects of geometric design and signal control. By this way, the capacity of vehicles at CFI will be enhanced accordingly. The rest of this paper is organized as follows. The potential conflicts of conventional CFI design and the countermeasures geometric design are introduced in Section 2. Section 3 presents the linear-program optimization model for the signal control. A case study is used to validate the optimization effectiveness for this design in Section 4. Section 5 performs sensitivity analyses to identify its best application domain. Conclusions and recommendations are given at the end of the paper.

2. Geometric design

2.1. Potential conflict analysis

Conventional geometric design of the continuous flow intersection is shown in Figure 1. The pre-signal is set at the upstream of the main-signal so that left-turn vehicles can be

moved to left-turn lanes on the left of the exit lanes, which can avoid the conflicts between left-turn and through vehicles at the main-signals. However, since the main-signals at CFI run in two phases, there are conflicts between left-turn bicycles and through vehicles if the left-turn bicycles turn left directly, as shown in Figure 1(a). If a two-step crossing rule is used for left-turn bicycles, it will cause conflicts between left-turn bicycles and left-turn vehicles, as shown in Figure 1(b). Because the left-turn bicycles need to cross a number of vehicle lanes, it not only causes severe safety risks to the bicycles but also leads to serious interference to the operation of the through vehicles. Therefore, eliminating the conflicts between left-turn bicycles and through vehicles at CFI is one of the key problems in promoting its application. In the following analysis, it is assumed that the left-turn bicycles turn left directly for the conventional design, which is a common rule for left-turn bicycles.

2.2. Proposed improved geometric design

As shown in Figure 2, to eliminate conflicts between left-turn bicycles and through vehicles, a pre-stop line for through vehicles and a crossing passage for left-turn bicycles are set at the pre-signal point of the CFI, and a left-turn bicycle lane is set between vehicle exit lanes and left-turn lanes. According to the path for left-turn bicycles, as shown in Figure 2 (red dotted line), left-turn bicycles can turn left directly at the main-signal after they enter the special left-turn bicycle lane form the roadside during the left-turn phase at the pre-signal. The left-turn and through vehicles and the left-turn bicycles are all controlled by the pre-signal. Therefore, the conflicts between left-turn bicycles and through vehicles can be eliminated by providing a special path in such design while maintaining a two-phase signal control at main-intersection and sub-intersections.

For the sake of fair comparison, in this paper, it is assumed the total widths of the traffic lanes used for vehicles and bicycles before and after the optimization design are equal. The left-turn bicycle lanes, which are highlighted in blue, can be provided by reducing the widths of the bicycle lanes at the roadside.

Please note to ensure the left-turn vehicles and through vehicles can be served in a single green phase, the CFI is usually deployed symmetrically at the two opposing approaches (Xuan, Daganzo, and Cassidy 2011). Although a two-way CFI design is used as an example to introduce the design idea, the proposed design can be applied in one or multiple legs with CFI. Therefore, no matter it is a two-way CFI (four approaches with CFI) or a one-way CFI (two opposing approaches with CFI), the proposed design can be used.

3. Signal control model

Grounded on the geometric design in Section 2, an optimal signal timing model is developed to further improve the vehicular capacity.

3.1. Notations

To facilitate the model presentation, notations used hereafter are summarized in Table 1. They are divided into three categories: parameters (model inputs), decision variables (model outputs), and auxiliary variables. Figure 3 illustrates the layout of key geometric parameters.

3.2. Objective function

The proposed model aims to maximize the practical capacity of the CFI (Allsop 1972), as shown in Eq. (1). Please note that traffic volume of each movement on each leg (q_{iw}) is given as outside input. It indicates that the turn proportions would remain constant

(Gallivan and Heydecker 1988; Wong and Wong 2003a, 2003b; Wong and Heydecker 2011).

$$\max \quad \sum_{i=1}^{4} \sum_{w=1}^{3} \mu q_{iw} \tag{1}$$

3.3. Constraints

3.3.1 Phase plan

As illustrated in Figure 4, the main-signal of the CFI is controlled by two phases, including east-west direction and south-north direction, which can be specified in Eq. (2)-(5). Without loss of generality, the start of green for the east-west direction is set to be 0. The pre-signal is also controlled by two phases including through phase for through and exit movements and left-turn phase for left-turn vehicles and bicycles, which can be specified in Eq. (6)-(8). To coordinate the main-signal and pre-signal, the starting time of green light at the main-signal in the east-west direction is required to be the same as the starting time of the through phase for through and exit movements at the pre-signal on the east and west leg. Along the same line, the main-signal in the east-west direction is required to be the same as the starting time of the through phase for through and exit movements at the pre-signal on the east and west leg, which can be specified in Eq. (9). There are two reasons why the pre-signal and through green start at the same time (see phases 1 and 3 in Figure 4). The first reason is that the through vehicles can enter the approach lanes and pass the intersection by following the vehicles in front as soon as the main-signal turns to green, which can ensure the operational efficiency of the intersection. The second reason is that some left-turn and right-turn vehicles from adjacent approaches will be queueing between the pre-signal and main-signal because the left-turn vehicles should enter the left-turn lanes before the start of green of the main-signal (see phases 2 and 4 in Figure 4). Therefore, the green time can

be used to clear the queuing vehicles between the pre-signal and main-signal while vehicles are approaching the pre-signal at the exit.

If a one-way CFI (two opposing approaches with CFI) is used, the phase plan of the approaches without the CFI should be replaced by a conventional phase plan. Please note the setting of through phases following left-turn phases is very much a matter of practice, which can provide sufficient time for the left-turn vehicles from the CFI approach to enter the left-turn lanes before the start of green of the main-signal.

$$g_i = 0,\ \forall i \in \{1,3\} \tag{2}$$

$$g_{i+1} = g_i + \lambda_i + I\xi,\ \forall i \in \{1,3\} \tag{3}$$

$$\lambda_i = \lambda_{i+2},\ \forall i \in \{1,2\} \tag{4}$$

$$\lambda_i + \lambda_{i+1} + 2I\xi = 1,\ \forall i \in \{1,3\} \tag{5}$$

$$g^p_{iw} = g^p_{i(w+1)} + \lambda^p_{i(w+1)} + I\xi,\ \forall i \in \{1,3\}, w = 1 \tag{6}$$

$$g^p_{iw} = g^p_{i(w+1)} + \lambda^p_{i(w+1)} + I\xi - 1,\ \forall i \in \{2,4\}, w = 1 \tag{7}$$

$$\lambda^p_{iw} + \lambda^p_{i(w+1)} + 2I\xi = 1,\ \forall i \in \mathcal{L}, w = 1 \tag{8}$$

$$g^p_{iw} = g_i,\ \forall i \in \mathcal{L}, w \in \{2,4\} \tag{9}$$

3.3.2 Cycle length

To coordinate the main-signal and pre-signal, the main-signal cycle length of the intersection should be the same as that of the pre-signal and within the reasonable range of maximum and minimum cycle length. Besides, to ensure that the established model is a linear model (Wong and Wong 2003a, 2003b; Wong and Heydecker 2011), instead of

defining the cycle length directly as the control variable, its reciprocal $\xi = 1/C$, is adopted, as given by Eq. (10).

$$\frac{1}{C_{min}} \geq \xi \geq \frac{1}{C_{max}} \tag{10}$$

3.3.3 Minimum green time

Conventionally, the green time of each vehicular movement should meet the minimum green time requirement at both main-signal and pre-signal, as shown in Eq. (11) and (12), respectively.

$$\lambda_i \geq G_{\min}\xi, \ \forall i \in \mathcal{L} \tag{11}$$

$$\lambda_{iw}^{p} \geq G_{\min}\xi, \ \forall i \in \mathcal{L}, w \in \{1,2,4\} \tag{12}$$

Considering the operation characteristics of bicycles, the green time should also meet the requirements of the bicycle crossing time at both main-signal and pre-signal, as shown in Eq. (13) and (14), respectively. As shown in Figure 5, it should be longer than the sum of the queue clearance time of bicycles waiting in line during the red light and the clearance time of bicycles at the end of green.

$$\lambda_i \geq G_{bi} + I_{bi}\xi, \ \forall i \in \mathcal{L} \tag{13}$$

$$\lambda_{iw}^{p} \geq G_{biw}^{p} + I_{biw}^{p}\xi, \ \forall i \in \mathcal{L}, w = 1 \tag{14}$$

The queue clearance time of bicycles waiting in line during the red light can be calculated based on the traffic wave theory (FHWA 2017; Knoop and Daamen 2017; Wierbos et al. 2018; Goñi-Ros et al. 2018). The bicycle aggregation wave during the red light is the transition from a high-speed and low-density state to a stopping state after the red signal starts, as given by Eq. (15). The bicycle dissipation wave during the green

light is the transition from a stopping state to a saturation flow state after the green signal starts, as given by (16). Thus, the queue clearance time of bicycles waiting in line at the main-signal and pre-signal can be calculated using (17) and (18). The two terms on the right side of the equations represent the time of dissipation wave propagating to the maximum queue and the time of bicycle at the end of the queue passing through the stop line, respectively.

$$u_{Aiw} = \frac{k_0 v_0 - k_a v_a}{k_0 - k_a} = \frac{q_{biw}}{k_0 - k_a},\ \forall i \in \mathcal{L}, w \in \{1,2\} \tag{15}$$

$$u_{Biw} = \frac{k_s v_s}{k_a - k_s},\ \forall i \in \mathcal{L}, w \in \{1,2\} \tag{16}$$

$$G_{bi} = \frac{u_{Aiw}(1-\lambda_i)}{u_{Biw} - u_{Aiw}} + \frac{u_{Aiw} u_{Biw}(1-\lambda_i)}{(u_{Biw} - u_{Aiw}) v_s},\ \forall i \in \mathcal{L}, w = 2 \tag{17}$$

$$G_{biw}^{p} = \frac{u_{Aiw}(1-\lambda_{iw}^{p})}{u_{Biw} - u_{Aiw}} + \frac{u_{Aiw} u_{Biw}(1-\lambda_{iw}^{p})}{(u_{Biw} - u_{Aiw}) v_s},\ \forall i \in \mathcal{L}, w = 1 \tag{18}$$

Due to the significant speed difference between bicycles and vehicles, sufficient clearance time should be set to ensure the safety of bicycles, which can be calculated according to the crossing passage width and the speed of bicycles. The bicycle clearance time at the main-signal and pre-signal can be calculated by Eq. (19) and (20), respectively.

$$I_{bi} \geq \frac{L_{biw}}{v_s},\ \forall i \in \mathcal{L}, w \in \{1,2\} \tag{19}$$

$$I_{biw}^{p} \geq \frac{L_{biw}^{p}}{v_s},\ \forall i \in \mathcal{L}, w = 1 \tag{20}$$

3.3.4 Queue length limitation of left-turn bicycles

To prevent the spillbacks in the displaced left-turn bicycle lane, the queue length of

bicycles should be no longer than the length of the left-turn lane, as given by Eq. (21).

$$L_i \geq \frac{q_{bi1}}{k_a \xi}, \ \forall i \in \mathcal{L} \tag{21}$$

3.3.5 Queue length limitation of vehicles

The phase plan used in the paper mainly ensures the proper coordination for the main-signal and pre-signal. However, a part of the vehicles may be trapped in the approach lanes after passing the pre-signal, or trapped in the exit lanes at the pre-signal after passing the main intersection. Therefore, the length of left-turn lanes (the length between the main-stop line and pre-stop line) should meet the following three constraints. First, it should be long enough to accommodate all the left-turn vehicles, as shown in Eq. (22). Second, it should be longer than the queue length of through vehicles trapped in the approach lanes after passing the pre-signal, as shown in Eq. (23). Third, it should be longer than the queue length of left-turn and right-turn vehicles from adjacent approaches trapped in the exit lanes after passing the main intersection, as shown in Eq. (24). To reduce the complexity of the model, the three constraints can be checked after the optimization. Moreover, in practice, the Do Not Block Intersection markings can be used to prevent the blockage caused by the vehicles' queue (FHWA 2009). It is assumed that users will obey the rule and do not block the main-intersection and sub-intersections.

$$L_i \geq \frac{q_{i1} h}{3600 \xi}, \ \forall i \in \mathcal{L} \tag{22}$$

$$L_i \geq \frac{q_{i2}\left(\lambda_{i2}^{p} - \lambda_i + \frac{L_i}{v}\xi\right)h}{3600 \xi \lambda_{i2}^{p}}, \ \forall i \in \mathcal{L} \tag{23}$$

$$L_i \geq \frac{\left(q_{(i-1)1} + q_{(i+1)3}\right)\left(\lambda_{i1}^{p} + \frac{L_i}{v}\xi\right)h}{3600 \xi \lambda_{(i+1)}}, \ \forall i \in \mathcal{L} \tag{24}$$

3.3.6 Saturation flow rate adjustment

The saturation flow rate at the main-signal and pre-signal can be calculated by Eqs. (25) and (26), respectively. According to the characteristics of this study, pedestrian-bicycle adjustment factor should be considered under the conventional CFI design in calculating the saturation flow rate at the main-signal, which can be determined based on the HCM2010 method (TRB 2010), as shown in Eqs. (27)-(30). Please note for the proposed design method, there is no need to adjust the saturation flow rate of through movement because the conflict between left-turn bicycles and through vehicles has been eliminated.

$$s_{iw} = s_{0iw} n_{iw} f_{iw},\ \forall i \in \mathcal{L}, w \in \mathcal{T} \tag{25}$$

$$s_{iw}^{p} = s_{0iw}^{p} n_{iw}^{p},\ \forall i \in \mathcal{L}, w \in \mathcal{T} \tag{26}$$

$$f_{iw} = 1 - OCC_{iw},\ \forall i \in \mathcal{L}, w \in \{1,2,3\} \tag{27}$$

$$OCC_{iw} = OCC_{piw} + OCC_{biw} - OCC_{piw} OCC_{biw},\ \forall i \in \mathcal{L}, w \in \{1,2,3\} \tag{28}$$

$$OCC_{piw} = \begin{cases} \frac{3600 q_{piw}}{2000} & \left(3600 q_{piw} \le 1000\right) \\ 0.4 + \frac{3600 q_{piw}}{1000} & \left(1000 \le 3600 q_{piw} \le 5000\right) \end{cases}, \forall i \in \mathcal{L}, w \in \{1,2,3\} \tag{29}$$

$$OCC_{biw} = \begin{cases} 0 & (q_{biw} = 0) \\ 0.02 + \frac{3600 q_{biw}}{2700} & (q_{biw} \ne 0) \end{cases},\ \forall i \in \mathcal{L}, w \in \{1,2,3\} \tag{30}$$

3.3.7 Degree of saturation

The degree of saturation of each traffic movement should be limited by a maximum acceptable value to ensure that the intersection operate reasonably well, so the constraints at the main-signal and pre-signal are shown as Eqs. (31) and (32) respectively.

$$\frac{\mu q_{iw}}{s_{iw}\lambda_i} \leq d_{\max},\ \forall i \in \mathcal{L}, w \in \{1,2,3\} \quad (31)$$

$$\frac{\mu q_{iw}}{s_{iw}^{p}\lambda_{iw}^{p}} \leq d_{\max},\ \forall i \in \mathcal{L}, w \in \{1,2,4\} \quad (32)$$

3.4. Solution

The optimization model presented above is a linear program with the objective function of Equation (1) and constraints (1)-(32), which can be readily handled by any commercial LP solver (e.g. Lingo).

4. Case study

4.1. The study site

To validate the optimization effects for this design, the intersection of Caitian Road - Fuhua Road in Shenzhen, China, was selected as a case for comparative analysis. At present, the north and south approaches of this intersection have adopted the design of CFI. The geometric and signal timing design scheme in practice are illustrated in the Figure 6(a) and (b), respectively. The surveyed average traffic demands during peak and no-peak hours are listed in Table 2. Since the capacity of the intersection increases with the increase of cycle length in general, for fair comparison, the upper limit for cycle length (maximum cycle length) in the optimization model is to the same level as the cycle length of the original plan, 120 s. The other design parameters are set as follows: the minimum cycle length is 60 s; the saturation flow rate of each direction is 1800 veh/h; the maximum acceptable degree of the saturation is 0.85; the speed of bicycles is 3.5 m/s; the clearance distances for bicycles at main-signal and pre-signal are 40 m and 30 m; according to the field survey, the bicycle arrival, stop, and departure densities are 0.02362, 0.55, and 0.3 bicycle/m.

4.2. Analysis plan

The optimal design method proposed in this paper was used to optimize the geometry and signal of this CFI, as shown in Figure 7. The microscopic simulation package Vissim 9 is used and calibrated as the unbiased evaluator to evaluate the performance of the proposed model in comparison with the original design. Since the original signal timing scheme under the original geometric layout may not be optimal under the investigation traffic demand, for fair comparison, the optimal signal timing scheme based on the original layout is added to analyze the performance of the proposed method. Therefore, the following three schemes were conducted for comparison. Scheme 1-original scheme (original layout + original signal timing), as shown in Figure6; Scheme 2-optimal design scheme (optimal geometric design + optimal signal timing), as shown in Figure 7; Scheme 3-optimal signal timing scheme based on the original layout (original layout + optimal signal timing), as shown in Figure 8.

4.3. Results and Discussions

Taking the throughput and delay as evaluation indicators, the simulation comparison results are shown in Figure 9. In the case of low traffic demand, the throughputs under the three schemes are the same as the input traffic demand, which indicates that all intersections under these three schemes were unsaturated, as shown in Figure 9(a). As shown in Figure 9(b), in the case of high traffic demand, the throughputs of the south and north legs in Scheme 1 and Scheme 3 are lower than the input traffic flow and this mean that the intersections had been oversaturated. However, the intersections in Scheme 2 can keep unsaturated under the high traffic demand condition, which indicates that the optimal design method proposed in this paper can improve the practical capacity of CFI by reducing the interference of left-turn bicycles on the

through vehicles.

Through further delay analysis (see Figure 9(c) and (d)), it was found that under the conditions of low and high traffic demand, the vehicular delay of Scheme 2 could be reduced by 25.5% and 50.8%, respectively, compared with Scheme 1. In addition, compared with Scheme 3, Scheme 2 could reduce the vehicular delay by 17.4% and 32.0%, respectively.

Compared with bicycle delay, it was found that under the condition of high traffic demand, the optimal design scheme could reduce bicycle delay by 19.9% and 7.8% compared with Scheme1 and Scheme 3, as shown in Figure 9(f). But under the condition of low traffic demand, the bicycle delay of the optimal design scheme was 1.4s higher than that of Scheme 3, basically maintaining the original level, as shown in Figure 9(e). Therefore, the optimal design scheme can reduce vehicle delay whether in the case of high traffic demand or low traffic demand. In addition, the interference between left-turn bicycles and through vehicles can be eliminated by changing the passing path of bicycles. The bicycle delay also can be reduced in the case of high traffic demand but it would increase slightly in the case of low traffic demand.

5. Sensitivity analyses

To further analyze the applicability of the proposed design method, sensitivity analysis was conducted for key parameters such as left-turn bicycle volume, through vehicle percentage, and cycle length. A full CFI (each of its four approaches containing a left-turn crossover) as shown in Figures 1 and 2 is used. The other design parameters are set the same as section 4. The left-turn bicycle volume was changed from 600 to 1500 bicycle/h, through vehicle percentage was changed from 0% to 65%, and the cycle length was changed from 80 to 120 s. Other parameters were consistent with the case study. The data used in the following analyses are calculated based on the proposed

model.

The effect of left-turn bicycle volume is analyzed by Figure 10(a). It can be seen from the figure that the practical capacity of vehicles decreases with the increase of the left-turn bicycles volume in the conventional design method while keeping its maximum level despite the increase of the left-turn bicycles volume in the optimal design method. On average, a 5% increase in the improvement of practical capacity can be obtained for every 100 left-turn bicycles per hour increase. This is mainly because in the conventional design method, the influence of bicycles on the capacity of through vehicles is positively correlated with the left-turn bicycle volume. However, in the proposed method, the conflict was eliminated. Therefore, the practical capacity is not affected although the through vehicles are additionally controlled by the pre-signal, because the green split of through movement at the pre-signal is generally no less than that at the main-signal.

The effect of through vehicle percentage is analyzed by Figure 10(b). It can be seen from the figure that the practical capacity of vehicles is almost the same in two design methods when the percentage of through vehicles is less than 40%; nevertheless, when the percentage of through vehicles is more than 40%, the proposed design begins to reflect its advantage in improving practical capacity. The improvement increases with the increase of through vehicle percentage. On average, a 3.5% increase in the improvement of practical capacity can be obtained for every 10% through vehicle percentage increase. This is mainly because left-turn will be the critical flow when the percentage of through vehicles is small, it would not affect the overall traffic volume at the intersection although left-turn bicycles reduce the saturation flow rate of through vehicles in conventional design. When the percentage of through vehicles increases and becomes the critical flow, the influence of bicycles on the practical capacity of through

vehicles causes the decrease of the overall practical capacity of the intersection. Therefore, the advantages of the proposed design are increasingly apparent.

The effect of cycle length is analyzed by Figure 10(c). It can be seen from the figure that the practical capacity of vehicles increases with longer cycle length at first and then levels off in both two design methods. The practical capacity of proposed design is higher than that of conventional design. The improvement of practical capacity decreases with the increase of cycle length and levels off. This is mainly because the growth rate of green split in each phase gained by the increase of the cycle length generally decreases with the increase of cycle length. Therefore, the longer the cycle length is, the less negative impact the left-turn bicycles have on the vehicle practical capacity, and the smaller the optimization effects of the proposed design method are.

6. Conclusions

An innovative design for left-turn bicycles at continuous flow intersections (CFI) is presented in this paper to eliminate the conflict between left-turn bicycles and through vehicles at the main-signal and to improve the overall practical capacity of CFI. From the perspective of the geometric design, the pre-stop line for through vehicles and the crossing passage for left-turn bicycles were set at the pre-signal points of the CFI. From the perspective of signal control, the control of the through vehicles at pre-signal was added. An optimization model was established to achieve the maximum practical capacity of vehicles with the consideration of many constraints, such as phase plan, cycle length, green time, and degree of saturation. The effectiveness and applicability for this design were validated by a case study and sensitivity analyses. The following conclusions can be drawn:

(1) The optimal design method proposed in this paper optimized the passing path of left-turn bicycles and signal control of the CFI. The general mechanism in

improving the practical capacity of vehicles is the elimination of the conflict between left-turn bicycles and through vehicles at the main signal.

(2) As for vehicles, this optimal design scheme can improve the practical capacity. Moreover, it can reduce the vehicular delay in the case of both high and low traffic demand, which indicates that the applicability of the proposed design method is wide enough. The improvements of practical capacity increase with the increase of the left-turn bicycles volume and through vehicle percentage, while decrease with longer cycle length. On average, a 5% increase and 3.5% increase in the improvement of practical capacity can be obtained for every 100 left-turn bicycles per hour increase and for every 10% through vehicle percentage increase, respectively.

(3) As for bicycles, the proposed method can reduce the delay in the case of high traffic demand and keep its original level in the case of low traffic demand.

Note that, there are some thresholds for the practical application of the design. First, according to the sensitivity analyses, from the point of operational efficiency, the proposed design begins to reflect its advantage when the percentage of through vehicles is more than 40%. Second, the application of the proposed design is on the basis that there is enough space to set the displaced left-turn bicycle lane, which can be achieved by narrowing the existing bicycle lanes at the roadside, which is possible because the left-turn cycling traffic will take another lane, or by widening the road slightly. Third, the proposed design does not deal with the conflicts between left-turning traffic (vehicles and bicycles) and pedestrians. To relieve the conflicts, the green of the left turn can start a little latter or end a little earlier than the through movement to provide the pedestrians a protected crossing time. To ensure the safety, adequate traffic barricades and colored pavements should be added for the left-turn bicycle lanes. The safety performance estimation and quantitative crash risk evaluation should be carefully

studied before the proposed design is perfected and implemented in the field, which is the direction of our future study.

Acknowledgements

The research is supported by the National Natural Science Foundation of China under Grant No. 51608324.

References

Al-Kaisy, A. F., and J. A. Stewart. 2001. "New approach for developing warrants of protected left-turn phase at signalized intersections." *Transportation Research Part a-Policy And Practice* 35 (6):561-74.

Allsop, Richard E. 1971. "SIGSET: a computer program for calculating traffic signal settings." *Traffic Engineering & Control* 13 (2):58-60.

Allsop, Richard E. 1972. "Estimating the traffic capacity of a signalized road junction." *Transportation Research* 6 (3):245-55.

Bagloee, S. A., and M. Asadi. 2016. "Crash analysis at intersections in the CBD: A survival analysis model." *Transportation Research Part a-Policy And Practice* 94:558-72.

Bai, L., P. Liu, C. Y. Chan, and Z. B. Li. 2017. "Estimating level of service of mid-block bicycle lanes considering mixed traffic flow." *Transportation Research Part a-Policy And Practice* 101:203-17.

Chang, Gang-Len, Yang Lu, and Xiangfeng Yang. 2011. "An Integrated Computer System for Analysis, Selection, and Evaluation of Unconventional Intersections." In. Baltimore, MD, United States: Maryland State Highway Administration.

Coates, A., P. Yi, P. Liu, and X. L. Ma. 2014. "Geometric and Operational Improvements at Continuous Flow Intersections to Enhance Pedestrian Safety." *Transportation Research Record* (2436):60-9.

DePrator, A. J., O. Hitchcock, and V. V. Gayah. 2017. "Improving Urban Street Network Efficiency by Prohibiting Conflicting Left Turns at Signalized Intersections." *Transportation Research Record* (2622):58-69.

Dong, S. X., Z. Yang, C. C. Xu, Z. Z. Tian, and P. Liu. 2016. "Multiobjective Evaluation of Left-Turn Waiting Areas at Signalized Intersections in China." *Transportation Research Record* (2553):138-49.

El Esawey, Mohamed, and Tarek Sayed. 2007. "Comparison of two unconventional intersection schemes: crossover displaced left-turn and upstream signalized crossover intersections." *Transportation Research Record* (2023):10-9.

El Esawey, Mohamed, and Tarek Sayed. 2011. "Operational performance analysis of the unconventional median U-turn intersection design." *Canadian Journal Of Civil Engineering* 38 (11):1249-61.

FHWA. 2009. *Manual on Uniform Traffic Control Devices*. Washington, DC: Federal Highway Administration (FHWA).

FHWA. 2017. "Revised Monograph on Traffic Flow Theory." In. Washington, DC, USA: Federal Highway Administration.

Foster, N., C. M. Monsere, J. Dill, and K. Clifton. 2015. "Level-of-Service Model for Protected Bike Lanes." *Transportation Research Record* (2520):90-9.

Gallivan, Stephen, and Benjamin Heydecker. 1988. "Optimising the control performance of traffic signals at a single junction." *Transportation Research Part B: Methodological* 22 (5):357-70.

Goñi-Ros, Bernat, Yufei Yuan, Winnie Daamen, and Serge Hoogendoorn. 2018. "Empirical Analysis of the Macroscopic Characteristics of Bicycle Flow During the Queue Discharge Process at a Signalized Intersection." In *Transportation Research Board 97th Annual Meeting*, 18-04103. Washington DC, United States: Transportation Research Board.

Goldblatt, R, F Mier, and J Friedman. 1994. "Continuous flow intersections." *ITE journal* 64 (7):35-42.

Goodno, M., N. McNeil, J. Parks, and S. Dock. 2013. "Evaluation of Innovative Bicycle Facilities in Washington, DC Pennsylvania Avenue Median Lanes and 15th Street Cycle Track." *Transportation Research Record* (2387):139-48.

Heydecker, Benjamin G, and Ian W Dudgeon. 1987. "Calculation of signal settings to minimise delay at a junction." *Transportation and Traffic Theory* 27 (1):159-78.

Hildebrand, Thomas E. 2007. "Unconventional intersection designs for improving through traffic along the arterial road." Florida State University.

Hughes, Warren, Ramanujan Jagannathan, Dibyendu Sengupta, and Joseph E Hummer. 2010. "Alternative intersections/interchanges: informational report (AIIR)." In. Washington, DC: Federal Highway Administration.

Improta, G, and GE Cantarella. 1984. "Control system design for an individual signalized junction." *Transportation Research Part B: Methodological* 18 (2):147-67.

Inman, Vaughan W. 2009. "Evaluation of signs and markings for partial continuous flow intersection." *Transportation Research Record: Journal of the Transportation Research Board* (2138):66-74.

Jagannathan, R., and J. G. Bared. 2005. "Design and performance analysis of pedestrian crossing facilities for continuous flow intersections." *Transportation Research Record* (1939):133-44.

Jagannathan, Ramanujan, and Joe G Bared. 2004. "Design and operational performance of crossover displaced left-turn intersections." *Transportation Research Record: Journal of the Transportation Research Board* (1881):1-10.

Jia, X. D., M. O'Mara, and M. Guan. 2007. "Rethinking geometric design standards for bike paths." *Journal Of Transportation Engineering-Asce* 133 (9):539-47.

Knoop, V. L., and W. Daamen. 2017. "Automatic fitting procedure for the fundamental diagram." *Transportmetrica B-Transport Dynamics* 5 (2):133-48.

Kothuri, S., K. Nordback, A. Schrope, T. Phillips, and M. Figliozzi. 2017. "Bicycle and Pedestrian Counts at Signalized Intersections Using Existing Infrastructure Opportunities and Challenges." *Transportation Research Record* (2644):11-8.

Liu, Pan, Jian John Lu, Huaguo Zhou, and Gary Sokolow. 2007. "Operational effects of U-turns as alternatives to direct left-turns." *Journal of Transportation Engineering* 133 (5):327-34.

Liu, Y., and Z. K. Luo. 2012. "A bi-level model for planning signalized and uninterrupted flow intersections in an evacuation network." *Computer-Aided Civil And Infrastructure Engineering* 27 (10):731-47.

Ma, Wanjing, Ye Liu, Jing Zhao, and Ning Wu. 2017. "Increasing the capacity of signalized intersections with left-turn waiting areas." *Transportation Research Part A Policy & Practice* 105:181-96.

Ma, Wanjing, Hanzhou Xie, Yue Liu, Larry Head, and Zhenke Luo. 2013. "Coordinated Optimization of Signal Timings for Intersection Approach with Presignals." *Transportation Research Record: Journal of the Transportation Research Board* (2355):93-104.

Majumdar, B. B., and S. Mitra. 2018. "Development of Level of Service Criteria for Evaluation of Bicycle Suitability." *Journal of Urban Planning and Development* 144 (2).

Mirheli, A., L. Hajibabai, and A. Hajbabaie. 2018. "Development of a signal-head-free intersection control logic in a fully connected and autonomous vehicle environment." *Transportation Research Part C-Emerging Technologies* 92:412-25.

Mohapatra, S. S., and P. P. Dey. 2018. "Estimation of U-Turn Capacity at Median Openings." *Journal of Transportation Engineering Part a-Systems* 144 (9).

Portilla, C., F. Valencia, J. Espinosa, A. Nunez, and B. De Schutter. 2016. "Model-based predictive control for bicycling in urban intersections." *Transportation Research Part C-Emerging Technologies* 70:27-41.

Providelo, J. K., and S. D. Sanches. 2011. "Roadway and traffic characteristics for bicycling." *Transportation* 38 (5):765-77.

Raihan, M. A., and P. Alluri. 2017. "Impact of Roadway Characteristics on Bicycle Safety." *Ite Journal-Institute of Transportation Engineers* 87 (9):33-40.

Silcock, JP. 1997. "Designing signal-controlled junctions for group-based operation." *Transportation Research Part A: Policy and Practice* 31 (2):157-73.

Suh, Wonho, and Michael P Hunter. 2014. "Signal design for displaced left-turn intersection using Monte Carlo method." *KSCE Journal of Civil Engineering* 18 (4):1140-9.

Sun, Weili, Xinkai Wu, Yunpeng Wang, and Guizhen Yu. 2015. "A continuous-flow-intersection-lite design and traffic control for oversaturated bottleneck intersections." *Transportation Research Part C: Emerging Technologies* 56:18-33.

Tanwanichkul, Ladda, Jumrus Pitaksringkarn, and Seksan Boonchawee. 2011. "Determining the Optimum Distance of Continuous Flow Intersection Using Traffic Micro-simulation." *Journal of the Eastern Asia Society for Transportation Studies* 9:1670-83.

Tengattini, S., and A. Y. Bigazzi. 2017. "Context-sensitive, first-principles approach to bicycle speed estimation." *Iet Intelligent Transport Systems* 11 (7):411-6.

Thompson, S. R., C. M. Monsere, M. Figliozzi, P. Koonce, and G. Obery. 2013. "Bicycle-Specific Traffic Signals Results from a State-of-the-Practice Review." *Transportation Research Record* (2387):1-9.

Tong, Y., L. Zhao, L. Li, and Y. Zhang. 2015. "Stochastic programming model for oversaturated intersection signal timing." *Transportation Research Part C-Emerging Technologies* 58:474-86.

TRB. 2010. *Highway Capacity Manual 2010*. Washington, DC: Transportation Research Board.

Webster, Fo Vo. 1958. "Traffic signal settings." In. London: H.M.S.O.

Wierbos, Maria J, Bernat Goñi-Ros, Victor L Knoop, and Serge Hoogendoorn. 2018. "Bicycle Queue Dynamics: Influence of Queue Density and Merging Cyclists on Discharge Rate at an Intersection." In *Transportation Research Board 97th Annual Meeting*. Washington DC, United States: Transportation Research Board.

Wong, Chi Kwong, and BG Heydecker. 2011. "Optimal allocation of turns to lanes at an isolated signal-controlled junction." *Transportation Research Part B: Methodological* 45 (4):667-81.

Wong, CK, and SC Wong. 2003a. "A lane-based optimization method for minimizing delay at isolated signal-controlled junctions." *Journal of Mathematical Modelling and Algorithms* 2 (4):379-406.

Wong, CK, and SC Wong. 2003b. "Lane-based optimization of signal timings for isolated junctions." *Transportation Research Part B: Methodological* 37 (1):63-84.

Wu, Jiaming, Pan Liu, Zong Z. Tian, and Chengcheng Xu. 2016. "Operational analysis of the contraflow left-turn lane design at signalized intersections in China." *Transportation Research Part C-Emerging Technologies* 69:228-41.

Xie, Chi, and Mark A Turnquist. 2011. "Lane-based evacuation network optimization: An integrated Lagrangian relaxation and tabu search approach." *Transportation Research Part C: Emerging Technologies* 19 (1):40-63.

Xuan, Yiguang, Carlos F. Daganzo, and Michael J. Cassidy. 2011. "Increasing the capacity of signalized intersections with separate left turn phases." *Transportation Research Part B-Methodological* 45 (5):769-81.

Yan, Chiwei, Hai Jiang, and Siyang Xie. 2014. "Capacity optimization of an isolated intersection under the phase swap sorting strategy." *Transportation Research Part B: Methodological* 60:85-106.

Yang, X. F., and Y. Cheng. 2017. "Development of signal optimization models for asymmetric two-leg continuous flow intersections." *Transportation Research Part C-Emerging Technologies* 74:306-26.

Yang, Z., P. Liu, Z. Z. Tian, and W. Wang. 2012. "Evaluating the Operational Impact of Left-Turn Waiting Areas at Signalized Intersections in China." *Transportation Research Record* (2286):12-20.

Yang, Z., P. Liu, Z. Z. Tian, and W. Wang. 2013. "Effects of Left-Turn Waiting Areas on Capacity and Level of Service of Signalized Intersections." *Journal of Transportation Engineering* 139 (11):1076-85.

You, Xiaoming, Li Li, and Wanjing Ma. 2013. "Coordinated Optimization Model for Signal Timings of Full Continuous Flow Intersections." *Transportation Research Record: Journal of the Transportation Research Board* (2356):23-33.

Yu, X. A., and P. D. Prevedouros. 2013. "Left-Turn Prohibition and Partial Grade Separation for Signalized Intersections: Planning-Level Assessment." *Journal Of Transportation Engineering-Asce* 139 (4):399-406.

Zhao, J., Y. Liu, and P. Li. 2016. "A network enhancement model with integrated lane reorganization and traffic control strategies." *Journal of advanced transportation* 50 (6):1090-110.

Zhao, J., Y. Liu, and T. Wang. 2016. "Increasing Signalized Intersection Capacity with Unconventional Use of Special Width Approach Lanes." *Computer-Aided Civil And Infrastructure Engineering* 31 (10):794-810.

Zhao, J., W. J. Ma, K. L. Head, and Y. Han. 2018. "Improving the operational performance of two-quadrant parclo interchanges with median U-turn concept." *Transportmetrica B-Transport Dynamics* 6 (3):190-210.

Zhao, J., W. J. Ma, K. L. Head, and X. G. Yang. 2015. "Optimal operation of displaced left-turn intersections: A lane-based approach." *Transportation Research Part C-Emerging Technologies* 61:29-48.

Zhao, Jing, Wanjing Ma, H. Michael Zhang, and Xiaoguang Yang. 2013. "Increasing the Capacity of Signalized Intersections with Dynamic Use of Exit Lanes for

Left-Turn Traffic." *Transportation Research Record: Journal of the Transportation Research Board* (2355):49-59.

Zhou, Y. P., and H. B. Zhuang. 2012. "Traffic Performance in Signalized Intersection with Shared Lane and Left-Turn Waiting Area Established." *Journal Of Transportation Engineering-Asce* 138 (7):852-62.

Table 1. Notations of key model parameters and variables.

Sets and Parameters	
$\mathcal{L}$	Set of legs
$i \in \mathcal{L}$	Index of legs, $i = 1,2,3,$ and 4 for east, south, west, and north leg, respectively, as shown in Figure 3
$\mathcal{T}$	Set of turning movements
$w \in T_i$	Index of turning movements on leg i, $w = 1, 2, 3, 4$ represents left-turn, through movement, right-turn, and exit movement, respectively, as shown in Figure 3
q_{iw}	Vehicular volume of movement w on leg i (veh/h)
q_{biw}	Bicycle volume of movement w on leg i (bicycle/s)
q_{piw}	Pedestrian volume of movement w on leg i (person/s)
C_{min}, C_{max}	Minimum and maximum cycle length (s)
I	Vehicular clearance time for a pair of conflicting traffic movements (s)
$G_{\min}$	Minimum green time limitation for vehicular movements (s)
v_0, v_a, v_s	Arrival, stop, and departure velocity of bicycles, respectively (m/s)
k_0, k_a, k_s	Arrival, stop, and departure density of bicycles, respectively (bicycle/m)
L_{biw}	Clearance distance for bicycles of movement w on leg i at the main-signal
L_{biw}^{p}	Clearance distance for bicycles of movement w on leg i at the pre-signal
L_i	Length of the left-turn lane (m)
h	Average space headway for queuing vehicles (m)
s_{0iw}	Base saturation flow rate per lane of movement w on leg i at the main-signal (veh/h/ln)
s_{0iw}^{p}	Base saturation flow rate per lane of movement w on leg i at the pre-signal (veh/h/ln)
n_{iw}	Number of lanes of movement w on leg i at the main-signal
n_{iw}^{p}	Number of lanes of movement w on leg i at the pre-signal
d_{max}	Maximum acceptable degree of the saturation
Decision Variables	

μ	Common flow multiplier of the intersection
ξ	Reciprocal of cycle length (1/s)
g_i	Start of green for leg i at main-signal, it is a fraction between 0 and 1 which expressed as the relative time in a signal cycle
g_{iw}^{p}	Start of green for movement w on leg i at pre-signal, it is a fraction between 0 and 1 which expressed as the relative time in a signal cycle
λ_i	Green time ratio for leg i at main-signal
λ_{iw}^{p}	Green time ratio for movement w on leg i at pre-signal
Auxiliary variables	
C	Cycle length (s)
G_{bi}	Queue clearance time of bicycles waiting in line during the red light on leg i at main-signal (s)
G_{biw}^{p}	Queue clearance time of bicycles waiting in line during the red light for movement w on leg i at pre-signal (s)
I_{bi}	Clearance time of bicycles between two phases on leg i at main-signal (s)
I_{biw}^{p}	Clearance time of bicycles between two phases for movement w on leg i at pre-signal (s)
u_{Aiw}, u_{Biw}	Aggregation and dissipation wave velocity of bicycles, respectively (m/s)
s_{iw}	Saturation flow rate of movement w on leg i at the main-signal (veh/h)
s_{iw}^{p}	Saturation flow rate of movement w on leg i at the pre-signal (veh/h)
f_{iw}	Pedestrian-bicycle adjustment factor of movement w on leg i at the main-signal
OCC_{iw}	Pedestrian-bicycle conflict zone occupancy of movement w on leg i
OCC_{piw}	Pedestrian conflict zone occupancy of movement w on leg i
OCC_{biw}	Bicycle conflict zone occupancy of movement w on leg i

Table 2. Traffic Demand.

Leg	Movement	Low traffic demand			High traffic demand		
		Vehicle (veh/h)	Bicycle (bicycles/h)	Pedestrian (p/h)	Vehicle (veh/h)	Bicycle (bicycles/h)	Pedestrian (p/h)
North	Left-turn	238	496	340	297	664	460
	Through	1060	228		1326	304	
	Right-turn	100	146		125	192	
South	Left-turn	55	446	160	69	587	215
	Through	1129	283		1412	372	
	Right-turn	138	131		172	172	
East	Left-turn	351	248	120	441	346	165
	Through	310	144		388	192	
	Right-turn	235	92		293	128	
West	Left-turn	451	336	345	564	398	465
	Through	399	208		498	280	
	Right-turn	118	112		148	160	

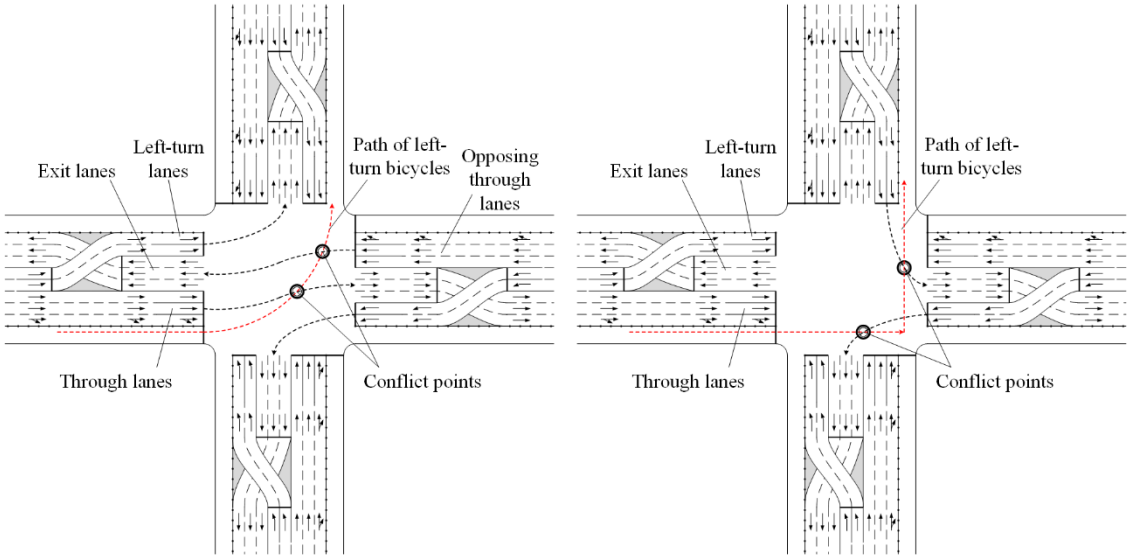

(a) One-step crossing rule for left-turn bicycles (b) Two-step crossing rule for left-turn bicycles

Figure 1. Potential conflicts for conventional design of CFI.

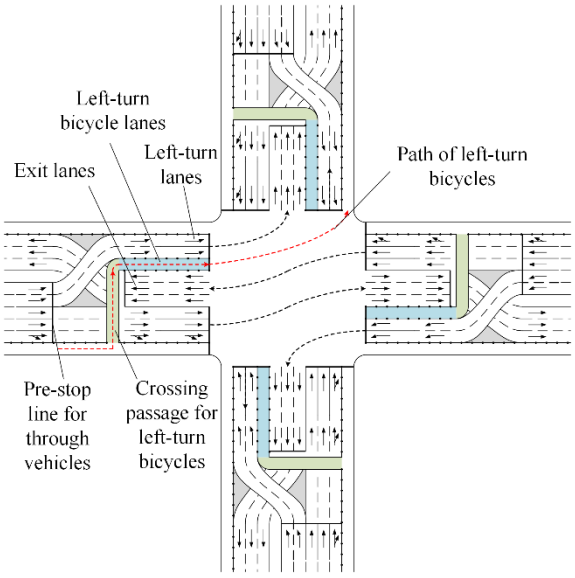

Figure 2. Proposed design of CFI.

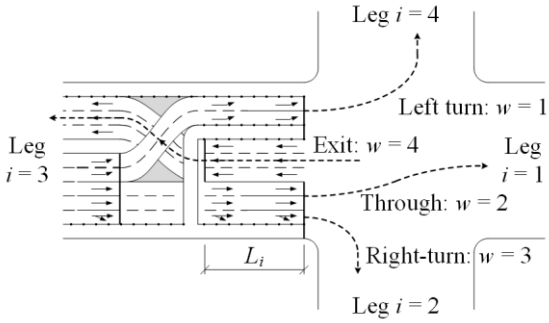

Figure 3. Schematic layout indicating the parameters.

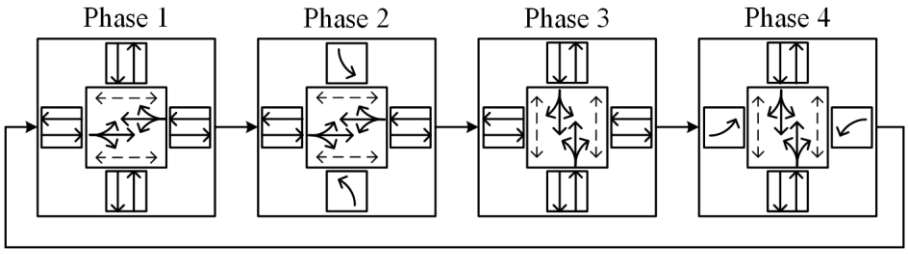

Figure 4. Phase plan.

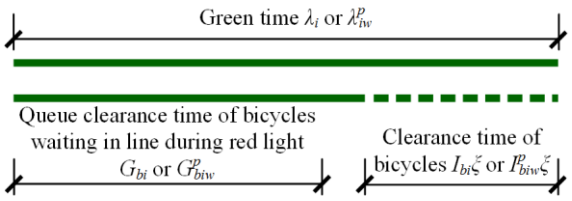

Figure 5. Minimum green time for bicycles.

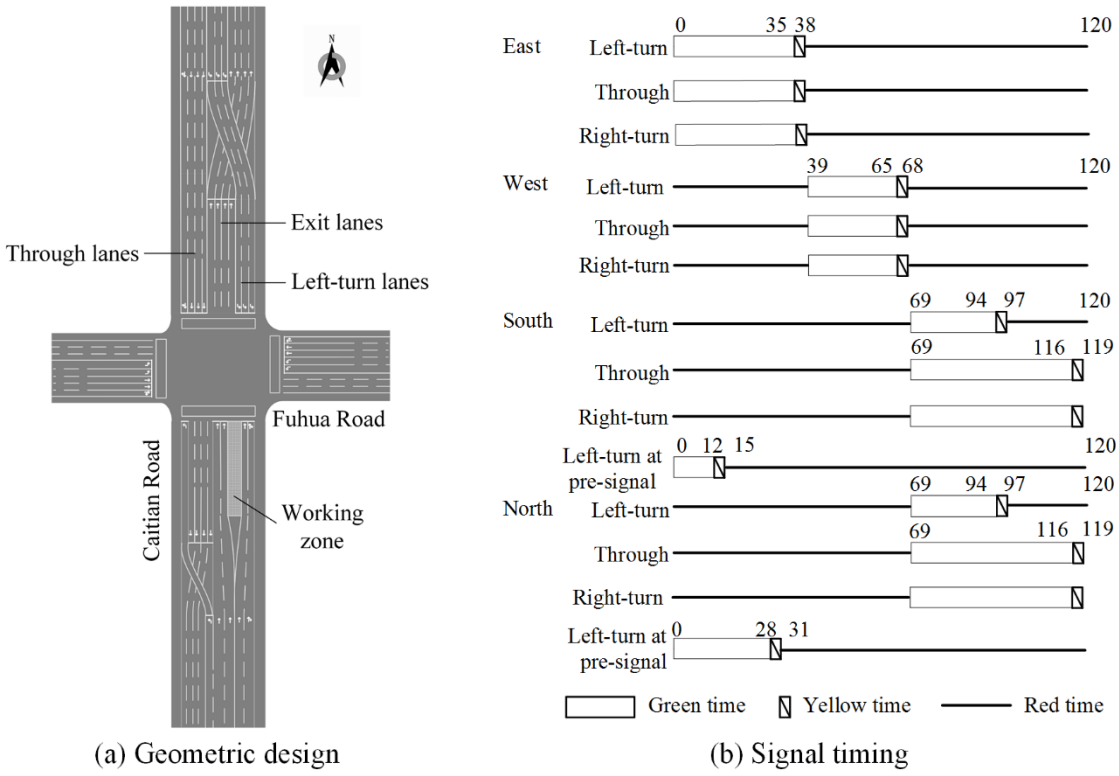

(a) Geometric design (b) Signal timing

Figure 6. Original Scheme of the case study (Scheme 1).

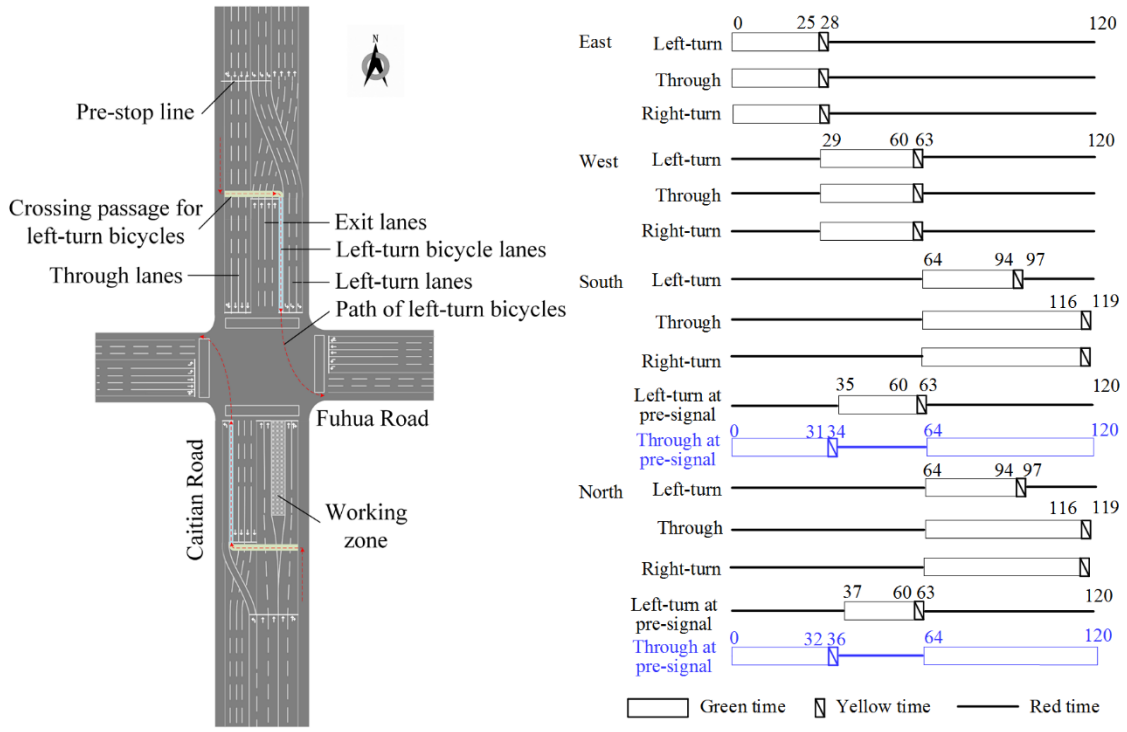

(a) Geometric design (b) Signal timing

Figure 7. Optimal Scheme of the case study (Scheme 2).

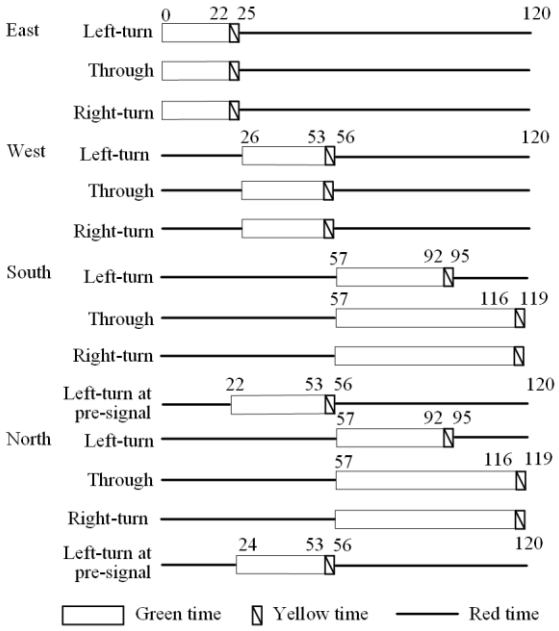

Figure 8. Optimal signal timing scheme based on the original layout (Scheme 3).

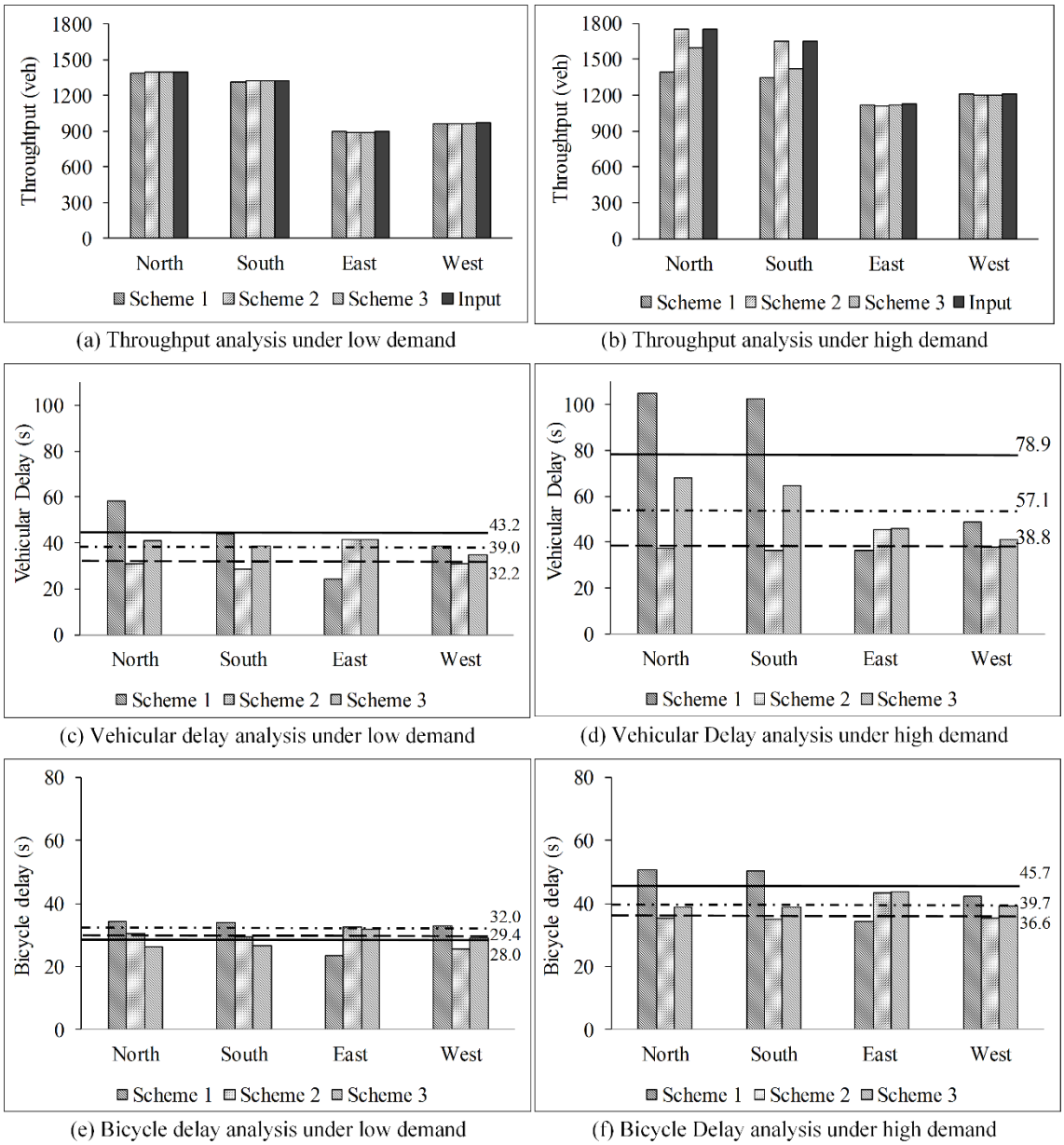

Figure 9. Comparison results.

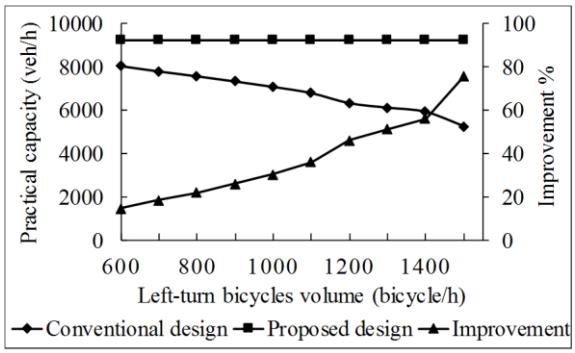

(a) Effect of left-turn bicycles volume

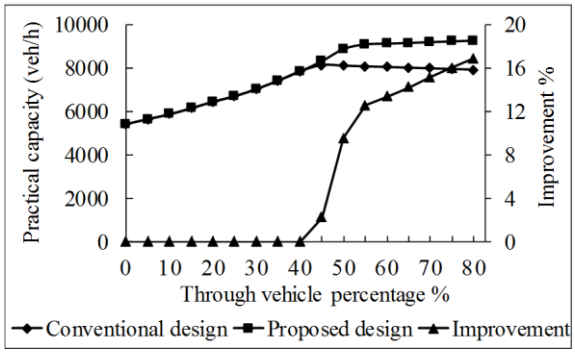

(b) Effect of through vehicle percentage

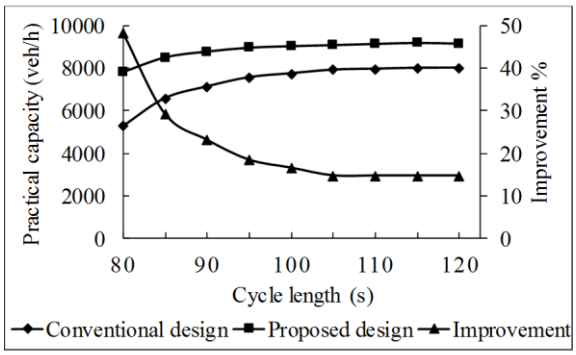

(c) Effect of cycle length

Figure 10. Results of sensitivity analyses.